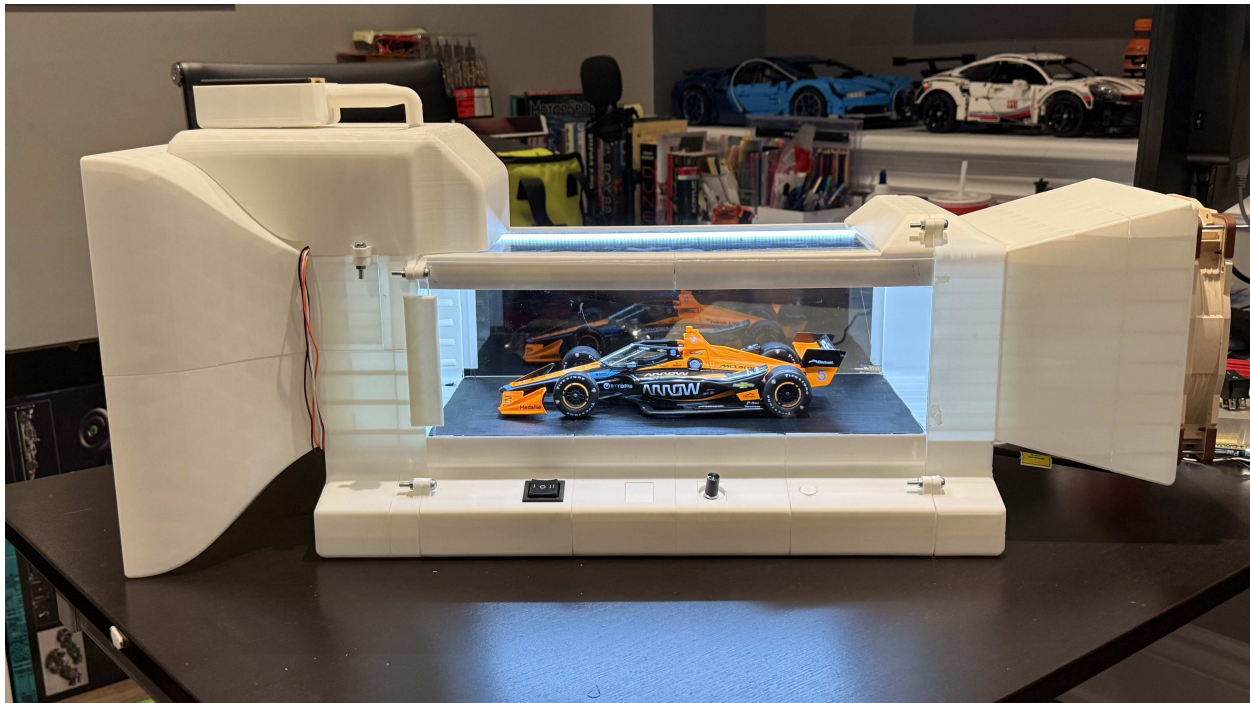


The Design Process and Qualitative Flow Analysis of a 1:18 Scale Homemade Wind Tunnel



Author:

Benjamin Sheng

December 28th, 2025

Abstract

This project aimed to design a functioning 1:18-scale wind tunnel capable of visualising streamlines around a model car. It has improved my computer-aided design, 3D printing, Arduino coding, and iterative design skills. This was followed by understanding how to optimise and improve the airflow visualised in the chamber.

The CAD phase involved designing multiple subsystems to work together in tandem while maintaining aesthetic appeal. This was followed by the electronics phase, in which I learned to wire servos, LEDs, buttons, and a PWM fan to an ESP32 board and code them to operate together. During the testing phase, I improved the wind-tunnel design in several areas, most notably the chamber. Substantial flow-optimisation work followed, as the initial flow was highly turbulent at best. All these components together make up the final product presented below.

This project also demonstrates the knowledge I gained through the Driver61 Aerodynamics course and *Race Car Aerodynamics* by Joseph Katz over the summer of 2025. The wind tunnel design was created in Fusion 360, and all 3D printing was performed on a Bambu Lab P1P. The parts were sourced from various websites.

Contents

Abstract	1
1 Introduction	3
2 Different Types of Wind Tunnels	4
2.1 Closed Return Wind Tunnel	4
2.2 Open Return Wind Tunnel	5
2.3 Catesby Tunnel	5
3 Wind Tunnel Working Sections	6
3.1 Blockage	6
3.2 $\frac{3}{4}$ Open	7
3.3 Slotted Walls	7
3.4 Adaptive Wall	8
4 Design	9
4.1 Project Constraints and Restrictions	9
4.2 Contraction	10
4.2.1 Servo Mounting and Housing	11
4.3 Chamber	12
4.4 Diffusion	13
5 Iterations	14
5.1 Flat vs. Angled Roof	14
5.2 Servo Mechanism	16
5.3 Electrics	16
5.4 Next Steps	17
6 Flow Analysis	18
6.1 Analysis at Different Speeds	18
6.2 Optimising Flow	22
7 Conclusion	29
8 Appendix	30
8.1 Figure List	30

1.0 — Introduction

This project was inspired by my love of aerodynamics and by a desire to visualise aerodynamic concepts such as streamlines, ground effect, and turbulence at a small scale. There is one essential aerodynamic testing tool in modern Formula One—the wind tunnel. So that's what I set out to replicate. In the end, this project strengthened my skills in computer-aided design, 3D printing, electrical work (soldering and crimping), iterative design, and aerodynamic flow analysis.

The following work is divided into four parts:

1. Learning about the different types of wind tunnels and their systems.
2. Detailed overview of my design process and preliminary CAD.
3. Detailed documentation of iterations made to the tunnel and next steps.
4. Chamber flow aerodynamic analysis.

The first phase of this project came from my completion of the Driver61 aerodynamics program and reading *Racing Aerodynamics: Designing for Speed* by Joseph Katz. This deepened my knowledge of the different types of wind tunnels and their associated advantages and disadvantages.

The second phase of this project was design. The entire wind tunnel was fully designed in Fusion 360, furthering my computer-aided design skills. Parts were manufactured using a Bambu P1P printer. This process taught me a lot about optimising a 3D printer and producing parts of the highest quality. Furthermore, with limited filament, I had to balance the trade-off between strength and weight by using different print patterns and infill levels. Post-manufacturing, I made iterations based on weaknesses identified during initial testing of the tunnel and its systems.

Finally, this report includes a detailed qualitative aerodynamic analysis of the streamlines displayed in the chamber. This analysis is once again based on my knowledge from the Driver61 aerodynamics program, from reading *Racing Aerodynamics: Designing for Speed* by Joseph Katz, and on additional research to understand airflow issues in the chamber. I provide a detailed analysis of the current flow's strengths, theories on the causes of its weaknesses, and potential solutions to optimise the airflow further.

2.0 — Different Types of Wind Tunnels

2.1 — Closed Return Wind Tunnel

This wind tunnel is most commonly used in modern Formula One. These tunnels form a closed system and are designed to recirculate the air within the chamber. An advantage of such a system is that it takes less energy to run the tunnel. Since the air is recirculated, it retains much of its energy, requiring less energy to bring it back up to speed before the chamber.



Figure 1: Ferrari Formula One Closed Return Wind Tunnel

The wind tunnel is rectangular, with turning vanes at each corner. Each side of the tunnel includes an expansion section to prevent air from accelerating as it recirculates. The fan, situated at the end of the loop, is followed by a honeycomb to streamline the newly energised air. This is then contracted (accelerated) before entering the chamber for use.

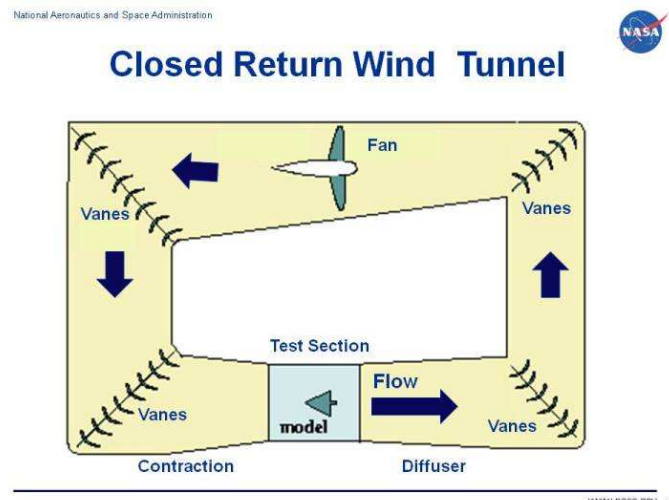


Figure 2: Closed Return Wind Tunnel Diagram

2.2 — Open Return Wind Tunnel

This wind tunnel is the easiest to set up and run. As air leaves the chamber, it naturally returns to its original state of contraction. The system is open, allowing continuous inflow of new air. This is the type of wind tunnel I have attempted to replicate.

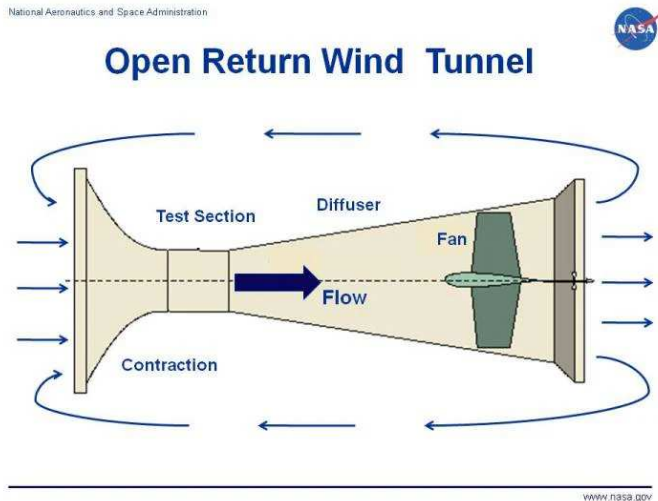


Figure 3: Open Return Wind Tunnel Diagram

2.3 — Catesby Tunnel

The Catesby Tunnel is an example of a wind tunnel that does not fit either description. A former railway tunnel, the Catesby is a 2.7-kilometre-long, purpose-built, straight road. The tunnel enables full-scale testing of a wide range of vehicles. The tunnel is sealed, ensuring a consistent environment across runs.



Figure 4: PIV in the Catesby Tunnel

3.0 — Wind Tunnel Working Sections

3.1 — Blockage

When an object is placed in a wind tunnel, the air must flow around the model. In an enclosed chamber, this is when problems start to grow. The tight space around the model causes it to flow faster and accelerate (air blockage). This acceleration can lead to inaccurate results. For example, if the wind speed is set to 10 m/s, it could be flowing at 11 m/s around the vehicle. Another type of blockage is wake blockage. Where the wake coming off the car or object disrupts the air's ability to flow around it. Once again, this leads to accelerated airflow, increased drag, and unreliable data.

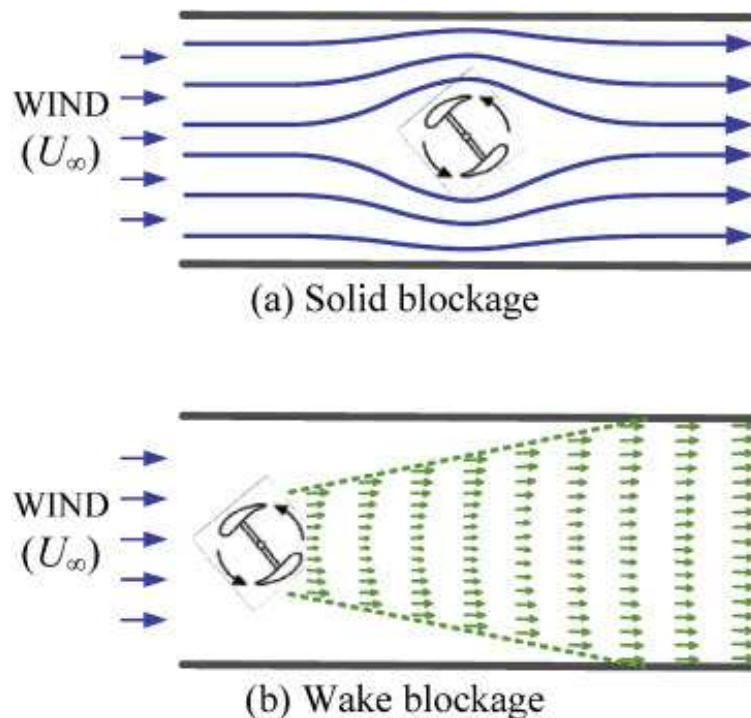


Figure 5: The Two Types of Blockage, Solid and Wake

To compensate for this issue, you can calculate the blockage factor, which is the ratio between the frontal surface area of your object and the cross-sectional area of the test section. You want to keep the blockage factor below 5-10% to maintain reliable results.

3.2 — $\frac{3}{4}$ Open

This type of wind tunnel has an entirely open working section. Usually used only for road-car and acoustics applications. It is suitable for assessing the flow underneath a vehicle. Blockage correction becomes almost negative.

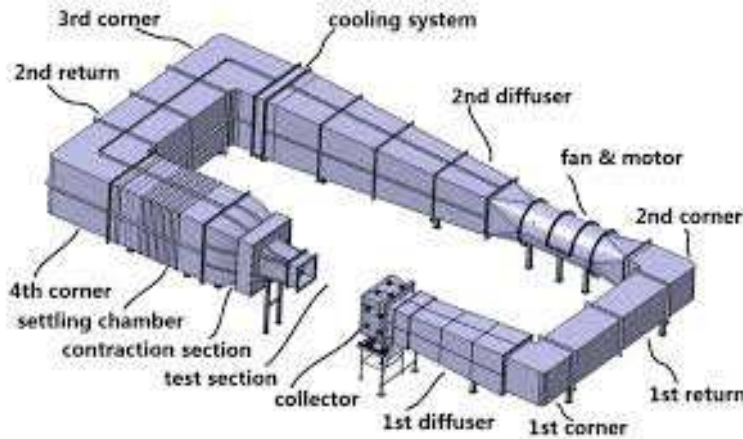


Figure 6: Diagram of a $\frac{3}{4}$ Open Wind Tunnel

3.3 — Slotted Walls

This type of wind tunnel has a working section with gaps (slots) between multiple components. This can lead to almost no blockage but tons of aero interference. Usually, full-scale models are used in this working section because they encounter many blockage issues.

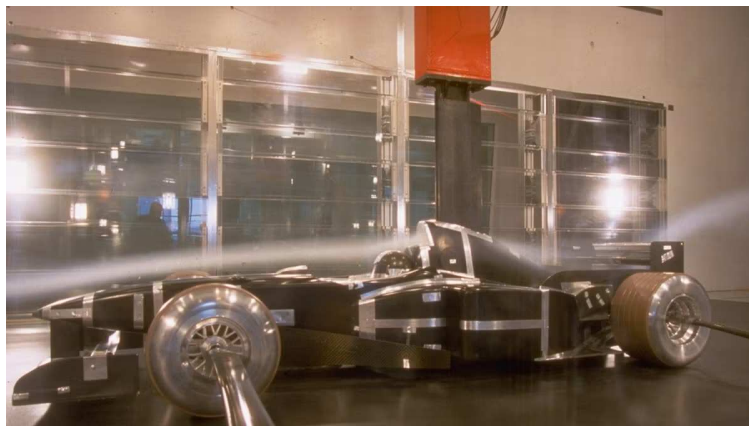


Figure 7: Slotted Wall Wind Tunnel

3.4 — Adaptive Wall

This type of wind tunnel has a working section where sections of the wall and ceiling are connected to motorised arms. These arms can be moved during the test to change the shape of the testing chamber and minimise airflow interference. Thus, this working section provides greater measurement accuracy.



Figure 8: Mercedes Adaptive Wall Wind Tunnel

4.0 — Design

4.1 — Project Constraints and Restrictions

There are many physical and material constraints of this project. First off, physical. The tunnel itself is pretty small. This is due to the limited space in my basement, as well as a personal preference for the project not to take up too much space and to be usable on a desk. This limits how streamlined the flow in the chamber can be. The short diffusion cone results in most vibrations from the spinning fan being strongly present in the chamber.

In terms of material constraints, the project is limited to the PLA used in the Bambu P1P printer. In many ways, this constraint is a positive, as 3D printing allows for a lot of freedom in terms of the types of shapes you can create. However, it once again limits the size of the tunnel as the bed is a limited size (265mm by 265mm). Furthermore, I do not want to use excessive material.

Electrically, the project runs on an ESP32 board and a wall outlet. The ESP32 board is quite voltage-limited, as it only accepts 3.3-5V and supplies a max of 5V. While it didn't really matter for this project, in future projects it may become a factor. In addition, only specific ports on the expansion board were programmable and could support the buttons, fan, and lights. Finally, I bought non-addressable LED lights. While this can be fixed by purchasing addressable ones, I ended up just leaving the lights on for the duration the tunnel was plugged in, instead of having a switch to turn them on and off. The fan was another constraint. I used a Noctua AF-20 fan, a 200mm PC fan (one of the largest on the market). The large fan diameter came at the cost of maximum fan RPM and thus wind speed.

A significant constraint was time. This project was completed in one month. This included everything from the final design to production and then the optimisation of the tunnel. During this one month, I also had a full-time summer job, which further reduced my working time. This taught me a lot about managing my time and being organised and direct with what I wanted to achieve every day.

4.2 — Contraction

The contraction sub-assembly is responsible for drawing air into the chamber and streamlining it. The prominent design feature of this sub-assembly is the cone. The cone is shaped to increase the speed of the air entering the chamber. Due to the tunnel's size, I cannot rely on a single large fan to generate high-speed airflow. We can increase the air speed by applying Bernoulli's Principle. The area of the cone reduces from 143 to 35 square inches. This contraction should increase the maximum air velocity from 8.2938 m/s (from just the fan pulling air) to 33.9 m/s (around 122 km/h). While conceptually this should increase the speed by a factor of 4, given the relatively thin cone depth and the open-loop system, the actual velocity increase is much lower.

The second layer of this subsystem is a 1-inch-thick round honeycomb. This is used to make all the air that is being sucked into the chamber laminar, allowing for better analysis of how aerodynamic parts affect the airflow around them.

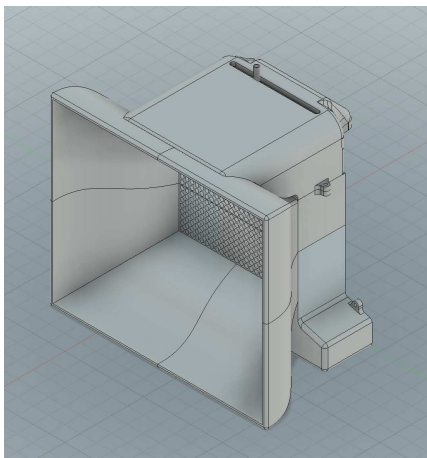


Figure 9: Contraction Assembly Isometric

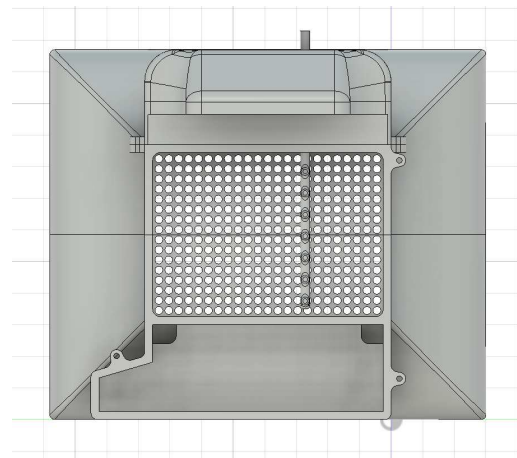


Figure 10: Contraction Assembly Front

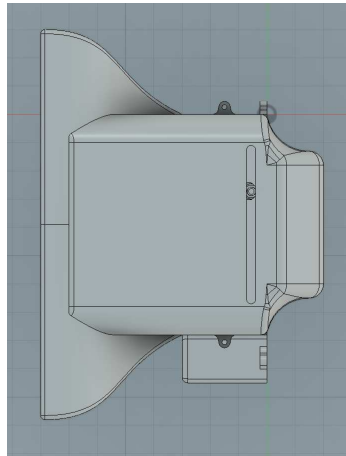


Figure 11: Contraction Assembly Top

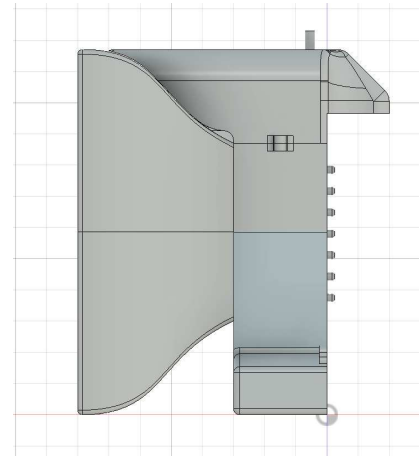


Figure 12: Contraction Assembly Right Side

4.2.1 — Servo Mounting and Housing

Smoke must be added to the air to visualise the airflow around a model. This subsystem within the contraction assembly is designed to do that. The design consists of a long smokestack with seven exits spread down the tube. This will enable an even distribution of smoke across the height of the chamber. A hobbyist smoke machine is used to pump smoke into the stack.

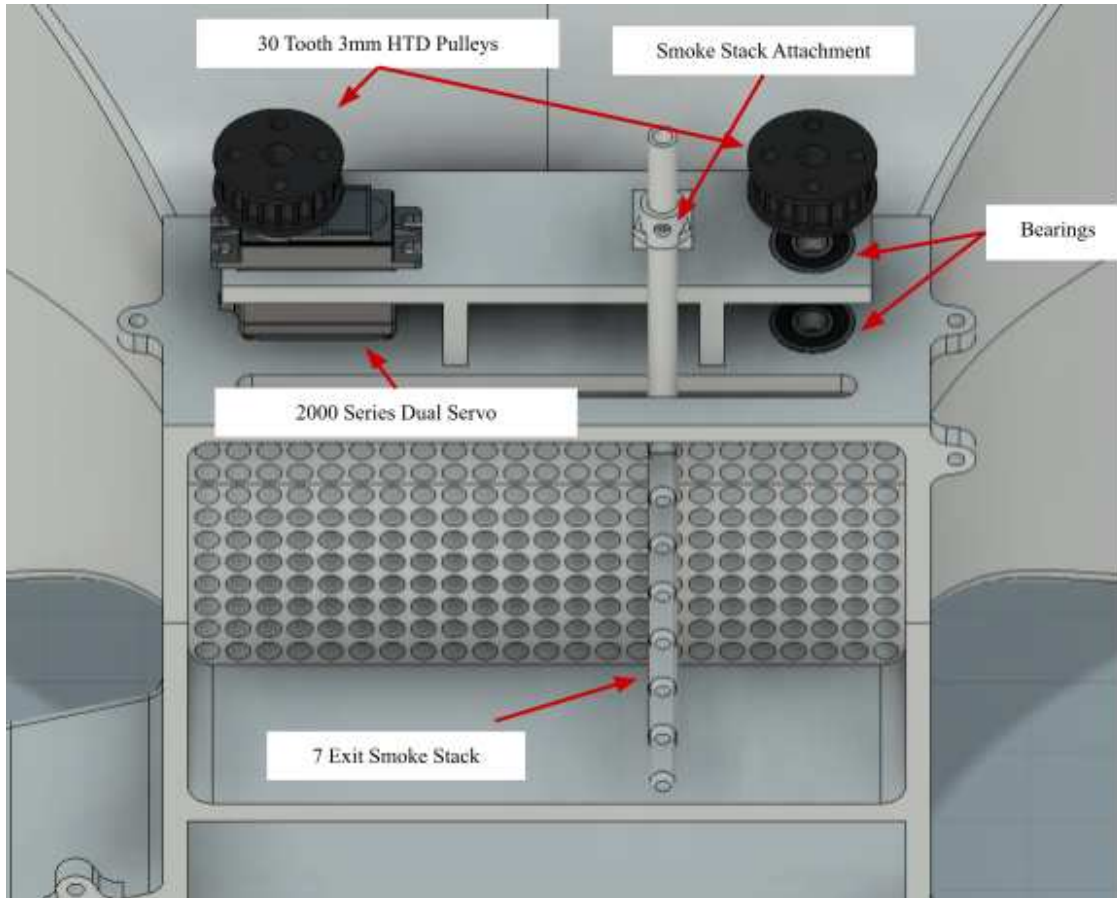


Figure 13: Servo Mechanism

Furthermore, the smokestack needed to be controlled from outside of the chamber, without stopping the test. This is not just a “cool” feature but rather a replication of industry practices. Efficiency when testing is key. During an era of limited testing, every second of runtime counts. A simple servo gear system moves the smokestack along a guide rail. A 2000-series dual-mode servo and two custom-designed 30-tooth, 3mm HTD belt pulleys comprise the system. An attachment clip on the smokestack hooks onto the timing belt, allowing it to slide. A 3-position rocker switch is mounted outside the chamber to control the smokestack.

4.3 — Chamber

The chamber has a testing platform of 15×7.5 inches and 6.5 inches tall. LED lights are along the angled sides of the roof. Clear 1/8 plastic panels can slide in and out to allow access to the chamber itself. There are cutouts on the front for all the switches. A maintenance cover at the back provides access to the chamber's Arduino system inside (underneath the platform). In this project, I used M4 screws to attach everything. An old version used dovetails, but this was scrapped due to its complexity.

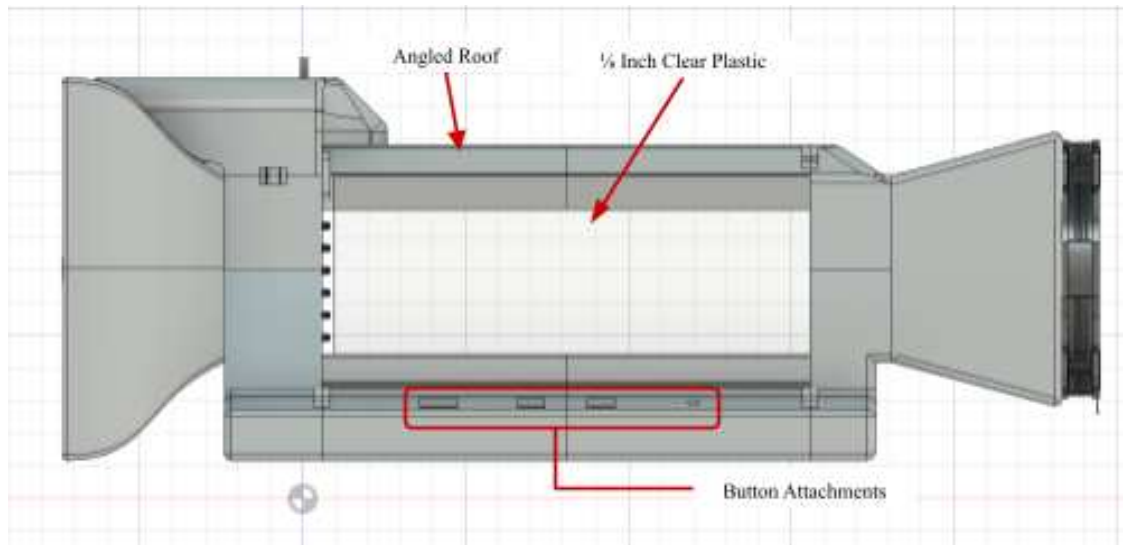


Figure 14: Testing Chamber Front

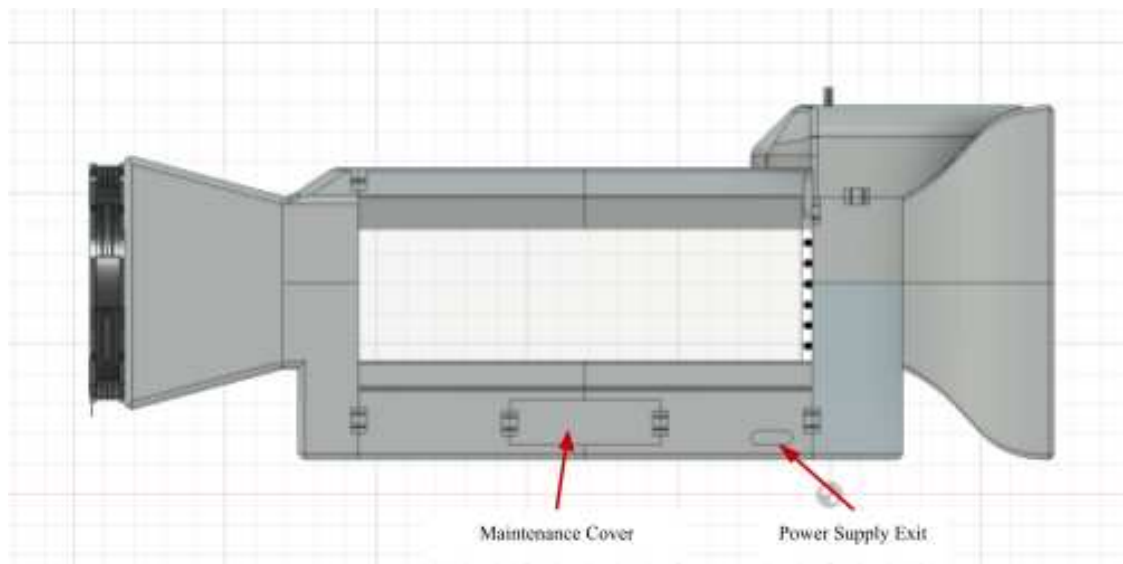


Figure 15: Testing Chamber Back

4.4 — Diffusion

The diffusion assembly is where the wind-tunnel fan is mounted. The fan used is a Noctua NF-A20, a PC cooling fan with a maximum RPM of 800 and a maximum wind speed of 8.2938 m/s, as predicted by Bernoulli's principle (see the contraction paragraph). A cone is bowed outward to accommodate the larger fan side, which is larger than the chamber cross-section. However, this also creates a lower pressure zone near the fan as the cross-section (area) increases. This allows for the fastest air speed in the chamber (Bernoulli).

Professional-grade large-scale tunnels typically have the air loop return to the contraction cone. Due to my size restrictions, I have chosen this non-looped tunnel design instead.

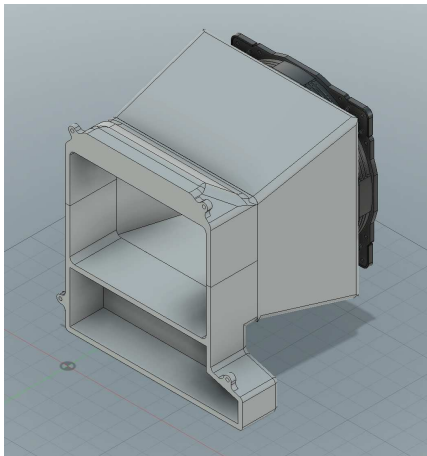


Figure 16: Diffusion Assembly Isometric

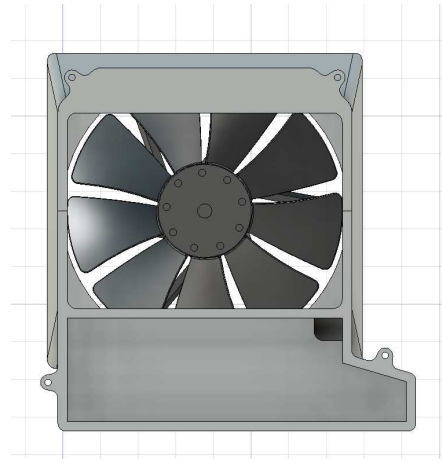


Figure 17: Diffusion Assembly Front

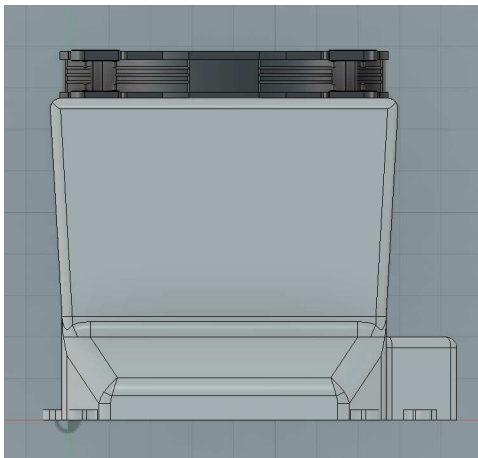


Figure 18: Diffusion Assembly Top

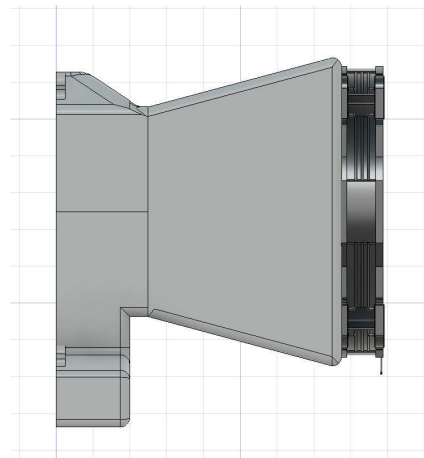


Figure 19: Diffusion Assembly Right Side

5.0 — Iterations

5.1 — Flat vs. Angled Roof

During initial testing, the airflow entering the chamber tended to rise straight up and become turbulent. This occurred with the four smoke exits near the top of the stack.

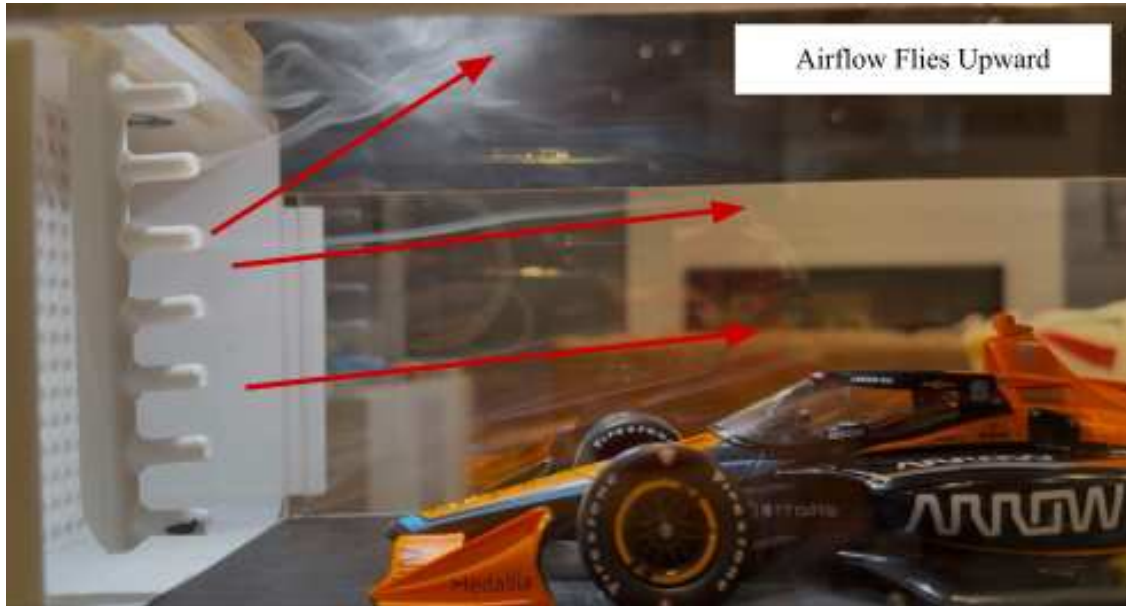


Figure 20: Airflow getting sucked up by an angled roof

My solution was to flatten the roof. With an angled roof, it was assumed that a low-pressure section at the top of the chamber drew the air up. The goal of this iteration was not to reduce turbulence, but to reduce the upward airflow motion as it enters the chamber. A flattened roof was installed and tested.

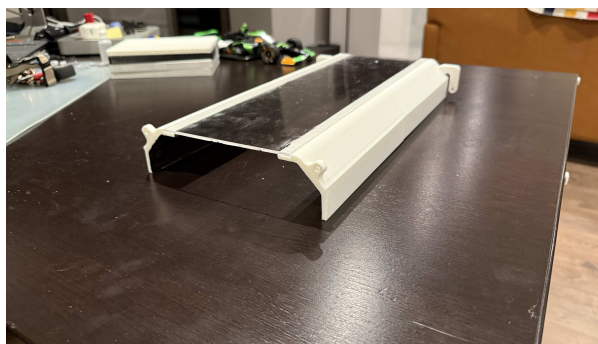


Figure 21: Diffusion Assembly Isometric



Figure 22: Diffusion Assembly Front

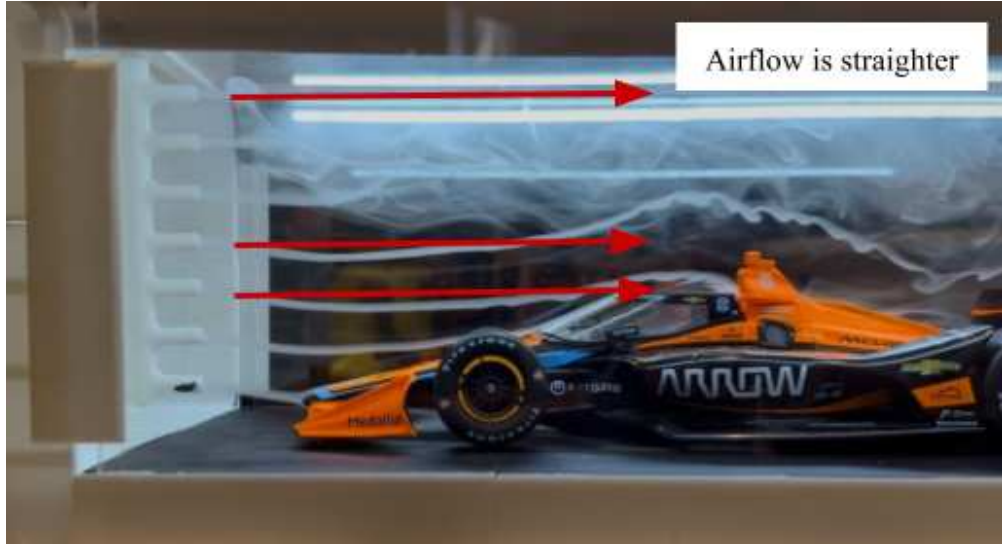


Figure 23: Airflow around model with flat roof

The results show airflow that remains quite turbulent, but the upward motion of the air is significantly reduced. Overall, this iteration was successful, and the turbulence can be attributed to the proximity of the fan to the chamber. These factors will be discussed in more depth in the tunnel flow analysis (section 6.0). While turbulence from the fan is a significant factor in the messy streamlines, another issue is an unsealed chamber. Smoke leaks from the smokestack in the servo housing and flows into the top of the chamber, interfering with airflow. By sealing the smokestack or the chamber (ideally both), some turbulence could be reduced.

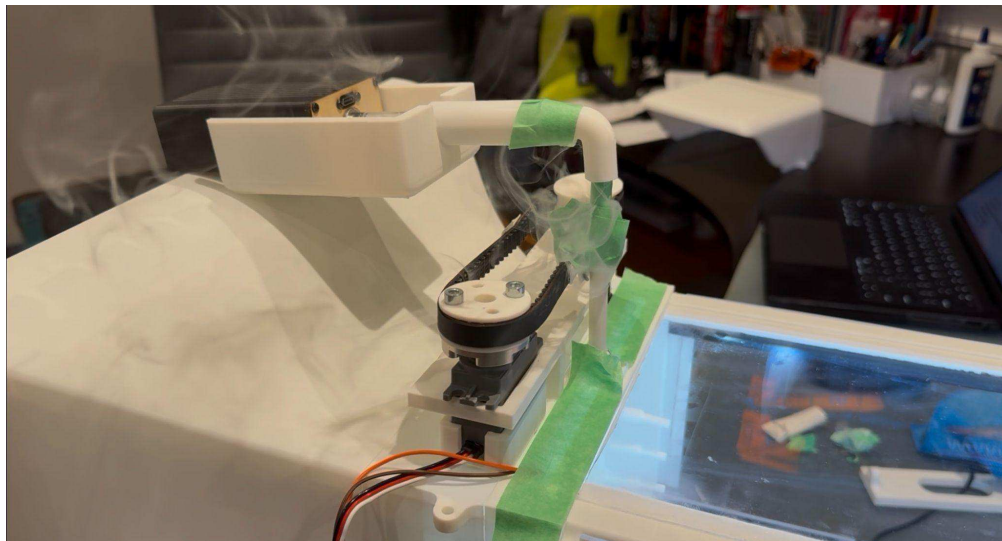


Figure 24: Smoke leaking out of the stack and flowing into the chamber

5.2 — Servo Mechanism

The first issue with the servo mechanism was that the mounting was excessively loose. The servo was not sturdy, and the entire mechanism swayed left to right. This was due to excessive tolerance in the design of the part that held the servo. My solution was to add a simple part to hold the servo in place. This was key in ensuring that the belt moved along the same line.

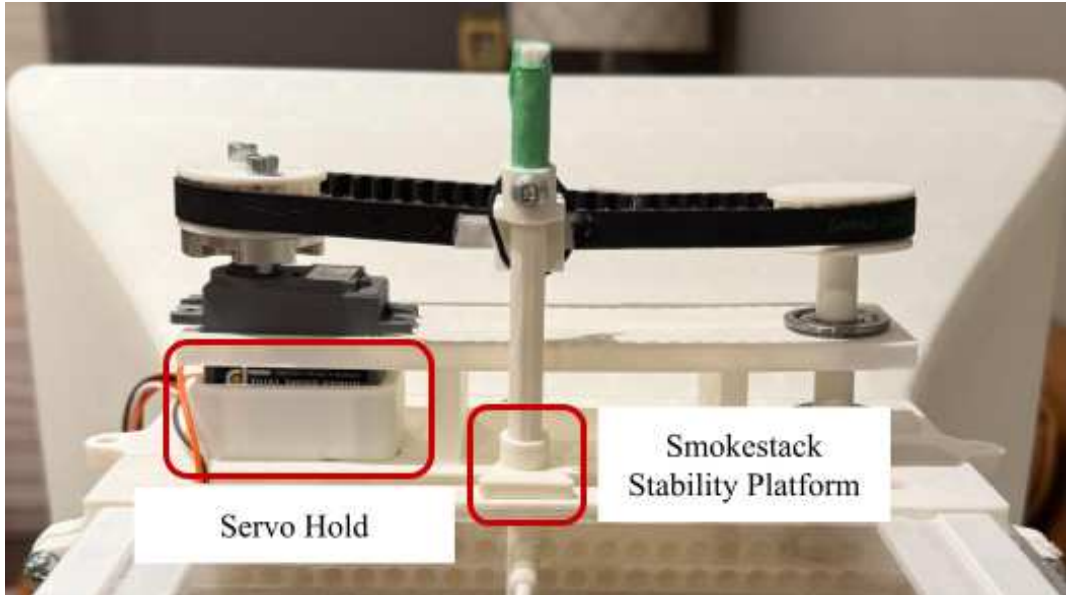


Figure 25: Servo hold and smokestack stability platform

The second issue that I encountered was the smokestack swaying left and right when the belt moved. This was because the smokestack itself was too loose and was not restrained by anything. It simply went wherever it wanted to in the slot. To fix this issue, I added a small platform that attached to the smokestack and slid along the top of the chamber with the stack. This allowed the smokestack to remain level as it transitioned from the left-most to the right-most position.

5.3 — Electrics

There were several issues with powering the Arduino and running LEDs to the chamber. The majority of these issues were due to voltage incompatibility or to buying parts that didn't work with my ESP32. Also, not purchasing addressable LEDs and then wondering why I couldn't control them like addressable LEDs. These are directly related to my inexperience with running a project like this. Many valuable lessons were learnt about how to make a project like this work seamlessly. In the end, these mistakes did increase the project's budget, but the lessons learnt made it worthwhile.

5.4 — Next Steps

There are many aspects of the wind tunnel that I would change. While the tunnel is technically finished, there are still many ways to improve it. Here is a list of action items and the justification for why:

Action Item	Justification
Upgrade the ESP32	The ESP32 had many limitations in terms of which ports were optimal for specific applications, as well as voltage limitations. A 3.3V to 5V range is workable, but a higher voltage would be better.
Create a return loop tunnel.	This would be quite a significant redesign, but one way to reduce fan vibrations in a relatively small space would be to create a return-loop tunnel. The fan would not affect the flow in the chamber, significantly reducing vibrations.
Extending the diffusion cone (move the fan farther away)	By extending the diffusion cone, this is another way to reduce fan vibration, simply by moving it farther away.
Higher fan speed	A higher fan speed would allow me to test how air flows around the model at those higher speeds. Replacing the large fan with four smaller ones would increase airflow and reduce vibrations in the chamber.
Finer entry and exit honeycomb	A finer-entry honeycomb would improve the streamlining of the air entering the chamber. While this was not our primary source of turbulence, it wouldn't hurt to have it.
Seal the chamber and smokestack.	During testing, I realised that smoke was leaking into the chamber from the entry mount and from open cracks in the smokestack itself. This may have added some turbulence in the airflow.
Slotted Walls	One way to reduce the blockage effect created by the small chamber's cross-sectional area is to add slotted walls. Allowing some air to escape and thus reducing the increase in velocity around the car.

6.0 — Flow Analysis

6.1 — Analysis at Different Speeds

The airflow in the wind tunnel's chamber is vital to determining its usability. The smoother the streamlines, the greater the qualitative results will be. Shown below is an analysis of the tunnel flow at different speeds and locations. The theoretical speeds given below are derived from the concept of steady incompressible flow through a varying area. So, through the equation, we know that:

$$A_1 v_1 = A_2 v_2 \quad (1)$$

$$v_2 = v_1 \frac{A_1}{A_2} \quad (2)$$

After rearranging the equation, we get that v_2 equals the initial velocity multiplied by the ratio of the areas. To calculate the initial air speed from just the fan, a simple relationship was derived from the fan tip speed (how fast the outer edge of the fan moves through air):

$$V_{tip} = \pi \times D \times \frac{N}{60}$$

For example, the Noctua NF-A20 200mm-diameter fan is running at 200 RPM. Putting this in the equation gets me a V_{tip} :

$$V_{tip} = \pi \times 0.2 \times \frac{200}{60}$$

$$V_{tip} = 2.093 \text{ m/s}$$

Inputting $V_{tip} = v_1$ in equation 1

$$v_2 = 2.093 \text{ m/s} \times \frac{143 \text{ in}^2}{35 \text{ in}^2}$$

The area reduces from 143 in^2 to 35 in^2

$$v_2 = 8.551 \text{ m/s} \times \frac{3600 \text{ s}}{1000 \text{ m}}$$

$$v_2 \cong 30.7836 \text{ km/h}$$

However, this is purely theoretical and would only hold if the same volumetric flow rate were to squeeze through a smaller area. In an open return tunnel like mine, this value is simply an upper bound. The values below are based on this upper bound of air speed; real values may be significantly lower.



Figure 26: Sideview, 25% Fan Speed(200RPM)



Figure 27: Front From Rear, 25% Fan Speed(200RPM)

1. 25% Fan Speed (200RPM) \cong 30 km/h

As shown in the figures, the flow at 25% fan power is quite streamlined at the bottom, but still rather turbulent at the top three nozzles. Due to the slow test speed, you can see quite a lot of interesting flow. For example, the streamlines all sag downward toward the chamber floor. Another interesting observation is the wobbly flow in the third and fourth flows from the bottom. This visualises the impact of the fan's vibrations on the streamlines. The flow does not come into contact with any objects, yet exhibits significant turbulence. We clearly observe airflow stalling in several regions: under the wheels and around the top of the halo. The low airspeed at this RPM is the main reason for the air stalling.



Figure 28: Sideview, 50% Fan Speed(400RPM)



Figure 29: Rearview, 50% Fan Speed(400RPM)

2. 50% Fan Speed (400RPM) \cong 61 km/h

The flow is more turbulent throughout the chamber, not just in the top three streamlines. The stalling around the side-pods and under the wheels alleviates itself as airspeed increases.

The streamlines are placed just off the side of the nose cone. This allows us to look at how the air is directed around the side of the car. The air flows through the suspension arms and is directed around the side pod undercut. You can also observe air directed beneath the floor, presumably via vortex generation.

We observe relatively poor airflow around the rear of the car. Flow is entirely detached from the side-pods and only just touches the rear wing, showing some downforce generation.



Figure 30: SideView, 100% Fan Speed(800RPM)



Figure 31: Front from Rear, 100% Fan Speed(800RPM)

3. 100% Fan Speed (800RPM) \cong 122 km/h

As shown in Figure 30, at 100% fan speed, the flow is a mess: turbulent everywhere, with nothing good to say. Both Figures 30 and 31 demonstrate the effect of the vibrations coming from the fan blades. In addition, the short diffusion cone and the absence of a fine mesh at the exit to reduce the amount of vibration entering the chamber further compound this.

6.2 — Optimising Flow

As shown below, the tunnel flow remains highly turbulent. There are three main factors for this:

1. Proximity of the fan to the chamber

The fan is approximately 7.5 inches away from the chamber. This proximity of the fan to the chamber prevents vibration from the fan from dissipating into the chamber. One way to reduce this is to turn the tunnel into a closed-loop tunnel, placing the fan parallel to the chamber, or increasing the length of the diffusion cone.

2. Fan diameter

Currently, the wind tunnel is driven by a single large 200mm PC fan. This induces significant vibrations that propagate into the chamber and affect the airflow. One way to reduce this is to replace the single large fan currently in use with four smaller fans. This would reduce vibrations entering the chamber and increase the maximum air speed.

3. Blockage

The ratio of the cross-sectional area of the chamber against the frontal area of the car is greater than 5 to 10%. This means that air accelerates faster around the vehicle because the walls confine it, leaving the air nowhere to go. A potential solution is to add slotted walls, which provide more space for air to circulate around the car.



Figure 32: Sideview, Airflow Turbulence

As mentioned in section 5.1 (Page 15), the change from an angled roof to a flatter roof over the chamber reduced the suction of air upwards. In addition to this iteration, I conducted extensive exit mesh testing to determine how to reduce turbulence caused by vibrations felt by the fan.

Meshing is the key to reducing much of the turbulence without extending the diffusion cone or reducing the fan diameter. The mesh breaks up large swirls, making the flow more straight. It does this by creating a gentle, uniform pressure drop across the chamber's cross-sectional area. That drop forces “fast” regions to slow down and “slow” regions to catch up, making the velocity profile flatter and the streamlines straighter. However, this will lead to pressure loss, which becomes more critical as the air speed increases.

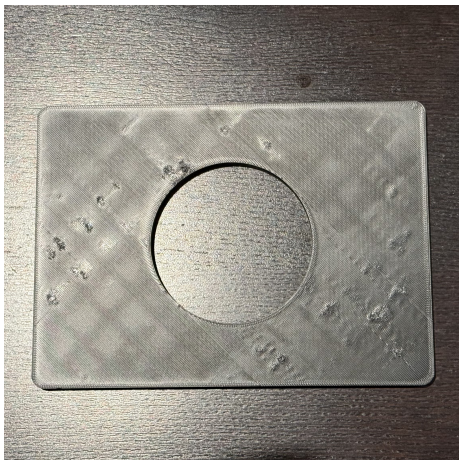


Figure 33: Simple Hole Exit Mesh

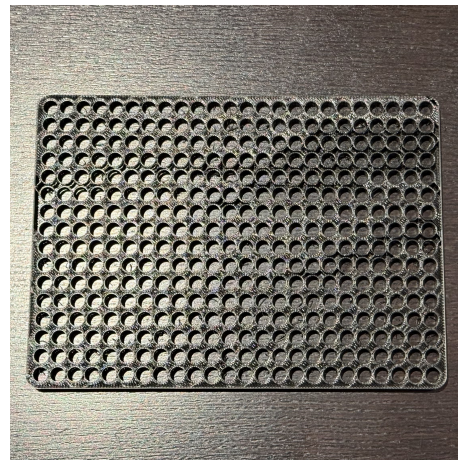


Figure 34: Coarse Exit Mesh



Figure 35: Bottom Half Exit Mesh

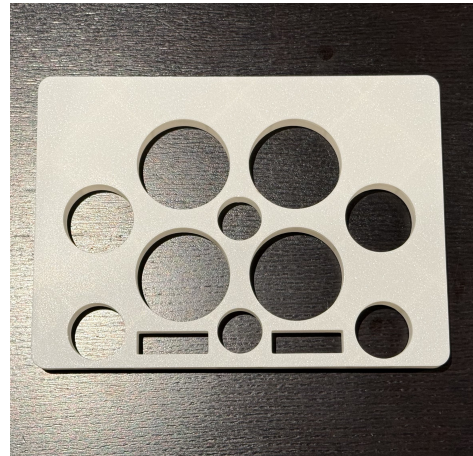


Figure 36: Final Exit Mesh

1. Simple Hole Exit Mesh

This was the first exit mesh that I tested. This simple hole reduces turbulence by making the flow more uniform. It pulls all the air towards the centre, allowing for more streamlined flow. This was simple yet effective, with ample room for improvement.

Airflow is quite streamlined until it reaches the model's roll hoop. Airflow still stalls under the wheels, but this is due solely to the slow fan speed. At high speed, the airflow remains highly turbulent throughout the chamber. However, the airflow is more closely attached to the engine cover and the rear wing. Furthermore, the turbulent flow is straighter and more organised than in the absence of this exit mesh.



Figure 37: Figure 33 Mesh, Slow Speed



Figure 38: Figure 33 Mesh, High Speed

2. Coarse Exit Mesh

A downside to the first mesh tested was its high-speed performance. A coarse mesh would allow lower pressure loss and better high-speed performance. It seems that my mesh wasn't coarse enough, because low-speed performance has improved significantly, whereas high-speed performance has worsened. The flow at low speed is quite attached to the model, and the turbulent swirls are pretty loose. The high-speed frame is particularly concerning, as there is no clear structure in the turbulence, and smoke appears to move wherever it wants. This indicates a high pressure loss at high speed, which is causing such poor flow.



Figure 39: Figure 34 Mesh, Slow Speed



Figure 40: Figure 34 Mesh, High Speed

3. Bottom Half Exit Mesh

The primary issue with the last mesh was the high-speed performance. This mesh was between a coarser mesh and a single hole, as in the first mesh. The slow-speed performance is quite similar. Flow is very streamlined, and turbulent swirls are loose as well. The high-speed flow has improved ever so slightly. The flow remains highly turbulent but exhibits greater directionality, with the majority of it seeking greater streamlining. This was quite a promising improvement and provides a direction for me to continue developing these meshes.



Figure 41: Figure 35 Mesh, Slow Speed



Figure 42: Figure 35 Mesh, High Speed

4. Final Exit Mesh

To improve on the previous mesh design, I increased the number of large circles (coarse mesh), raising the highest circle above the midpoint. The low-speed performance is quite similar to that of the third exit mesh tested. The flow does seem a bit messier, but this difference is minimal and can be attributed to the time at which the picture was taken. However, at high speed, it looks very similar to the second exit mesh tested. Turbulent air is moving in all directions with no overall direction. This iteration was clearly a step backwards.

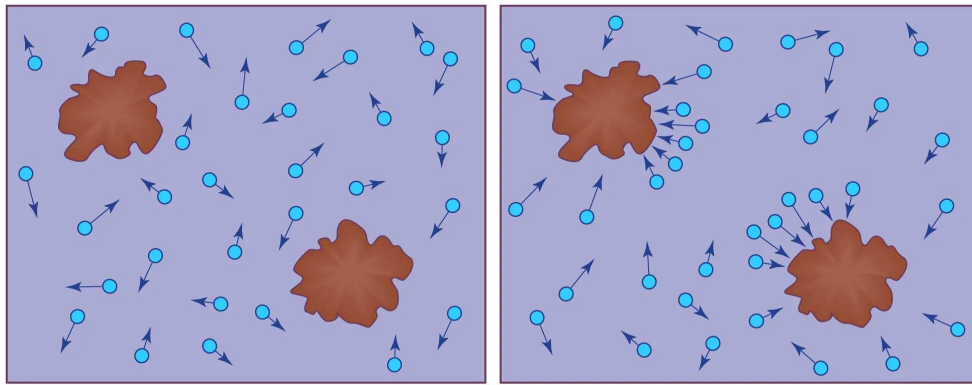


Figure 43: Figure 36 Mesh, Slow Speed



Figure 44: Figure 36 Mesh, High Speed

After all this testing, I concluded that it is best to have different meshes optimised for various speeds. At low speeds, a fine mesh allows for smoother airflow. At this low speed, the pressure loss from the mesh is relatively modest, making this a viable option. At higher speeds, a coarser mesh would create a similar effect with a similar pressure loss. This is because pressure loss increases with speed, leading to unwanted blockage. Overall, the Bottom Half Exit Mesh performed best at low speed, and the Simple Hole Exit Mesh performed best at high speed. However, the Bottom Half Exit Mesh strikes the best balance between low and high-speed performance.



© Encyclopædia Britannica, Inc.

Figure 45: Brownian motion demonstration

Despite all this testing, air is inherently turbulent. Brownian motion states that air molecules are travelling very fast and in all directions, even when the air is stationary. Furthermore, the boundary layer at the bottom of the tunnel and the shear forces from the model car make the air at the bottom of the tunnel more streamlined than at the top. If the fan speed were slowed so that the top flows were streamlined, the flow at the bottom would just fall to the ground. For these reasons, obtaining a perfect simulation in this setting is challenging.

7.0 — Conclusion

In conclusion, this project was very worthwhile and incredibly rewarding. I designed and built a 1:18-scale wind tunnel from concept to a finished product. Not only did I improve many practical skills, like advanced CAD modelling in Fusion 360, electronics integration using an ESP32, and systematic experimental testing, but I also gained a lot of knowledge about the theoretical concepts behind what makes a good wind tunnel—understanding how to optimise the tunnel and achieve the most streamlined airflow possible.

Throughout the design process, significant emphasis was placed on understanding how individual subsystems interact to influence overall tunnel performance. The contraction, chamber, and diffusion assemblies were designed as a cohesive system rather than as isolated components, and iterative modifications, such as transitioning from an angled to a flat roof and refining the smoke delivery mechanism, led to measurable improvements in flow behaviour.

The qualitative flow analysis revealed both the tunnel's strengths and limitations. After all iterations were completed, the wind tunnel at lower airspeeds produced relatively coherent streamlines, enabling clear visualisation of aerodynamic features around the model. At higher speeds, increased turbulence from fan proximity, vibration, blockage, and pressure losses becomes dominant. This demonstrates how different mesh geometries can be tuned to balance pressure loss and flow uniformity at various operating conditions. The struggles in this project helped me understand that in small-scale open-return tunnels, perfect flow conditions are unrealistic.

Overall, the completed wind tunnel serves not only as a functional experimental tool but also as a platform for continued development. With future upgrades such as improved diffusion length, reduced vibration, higher-speed fans, sealed flow paths, and alternative working-section configurations, the tunnel's performance and accuracy could be further enhanced. Most importantly, this project deepened my understanding of aerodynamics and reinforced the value of iterative design, making it a highly successful and rewarding engineering endeavour for a solo summer project under a tight timeline.

8.0 — Appendix

8.1 — Figure List

- Figure 1: Ferrari Formula One Closed Return Wind Tunnel
- Figure 2: Closed Return Wind Tunnel Diagram
- Figure 3: Open Return Wind Tunnel Pressure Diagram
- Figure 4: PIV used on a Jaguar in the Catesby Tunnel
- Figure 5: The Two Types of Blockage, Solid and Wake
- Figure 6: Diagram of a $\frac{3}{4}$ Open Wind Tunnel
- Figure 7: Slotted Wall Wind Tunnel
- Figure 8: Mercedes Adaptive Wall Wind Tunnel
- Figure 9: Contraction Assembly Isometric
- Figure 10: Contraction Assembly Front
- Figure 11: Contraction Assembly Top
- Figure 12: Contraction Assembly Right Side
- Figure 13: Servo Mechanism
- Figure 14: Testing Chamber Front
- Figure 15: Testing Chamber Back
- Figure 16: Diffusion Assembly Isometric
- Figure 17: Diffusion Assembly Front
- Figure 18: Diffusion Assembly Top
- Figure 19: Diffusion Assembly Right Side
- Figure 20: Airflow getting sucked up by an angled roof.
- Figure 21: Original angled roof
- Figure 22: Updated flat roof
- Figure 23: Airflow around model with flat roof
- Figure 24: Smoke leaking out of the stack and flowing into the chamber
- Figure 25: Servo hold and smokestack stability platform

- Figure 26: Sideview, 25% Fan Speed(200RPM)
- Figure 27: Front From Rear, 25% Fan Speed(200RPM)
- Figure 28: Sideview, 50% Fan Speed(400RPM)
- Figure 29: Rearview, 50% Fan Speed(400RPM)
- Figure 30: SideView, 100% Fan Speed(800RPM)
- Figure 31: Front from Rear, 100% Fan Speed(800RPM)
- Figure 32: Sideview, Airflow Turbulence
- Figure 33: Simple Hole Exit Mesh
- Figure 34: Coarse Exit Mesh
- Figure 35: Bottom Half Exit Mesh
- Figure 36: Final Exit Mesh
- Figure 37: Figure 40 Mesh, Slow Speed
- Figure 38: Figure 40 Mesh, High Speed
- Figure 39: Figure 41 Mesh, Slow Speed
- Figure 40: Figure 41 Mesh, High Speed
- Figure 41: Figure 42 Mesh, Slow Speed
- Figure 42: Figure 42 Mesh, High Speed
- Figure 43: Figure 43 Mesh, Slow Speed
- Figure 44: Figure 43 Mesh, High Speed
- Figure 45: Brownian motion demonstration